Molecular Membrane Biology, November–December 2004, **21,** 435–446

Taylor & Francis
healthsciences

The supramolecular structure of the GPCR rhodopsin in solution and native disc membranes

Kitaru Suda†, Slawomir Filipek‡, Krzysztof Palczewski#§¶, Andreas Engel† and Dimitrios Fotiadis†*

† M.E. Müller Institute for Microscopy, Biozentrum, University of Basel, CH-4056 Basel, Switzerland

‡ International Institute of Molecular and Cell Biology, Warsaw University, Warsaw, PL-02109, Poland

Departments of # Ophthalmology, § Pharmacology, and ¶ Chemistry, University of Washington, Seattle, WA 98195, USA

Summary

Rhodopsin, the prototypical G-protein-coupled receptor, which is densely packed in the disc membranes of rod outer segments, was proposed to function as a monomer. However, a growing body of evidence indicates dimerization and oligomerization of numerous G-protein-coupled receptors, and atomic force microscopy images revealed rows of rhodopsin dimers in murine disc membranes. In this work we demonstrate by electron microscopy of negatively stained samples, blue native- and sodium dodecyl sulphate-polyacrylamide gel electrophoresis, chemical crosslinking, and by proteolysis that native bovine rhodopsin exists mainly as dimers and higher oligomers. These results corroborate the recent findings from atomic force microscopy and molecular modeling on the supramolecular structure and packing arrangement of murine rhodopsin dimers.

Keywords: Blue native-polyacrylamide gel electrophoresis, cross-linking, G protein-coupled receptor, rhodopsin, transmission electron microscopy.

Abbreviations: 2-ME, 2-mercaptoethanol; AFM, atomic force microscopy/microscope; BN-PAGE, blue native-polyacrylamide gel electrophoresis; CCB, Coomassie brilliant blue G-250; DM, n-dodecyl-β-D-maltoside; DSP, dithiobis(succinimidyl propionate); DTT, dithiothreitol; EDTA, ethylene diamine tetra-acetic acid; GPCR, G protein-coupled receptor; HEPES, N-(2-hydroxyethyl) piperazine-N′-2-ethanesulfonic acid; LC-SPDP, succinimidyl 6-[3-(2-pyridyl-dithio)-propionamido]hexanoate; ROS, rod outer segment(s); SB, sample buffer; SDS-PAGE, sodium dodecyl sulphate-polyacrylamide gel electrophoresis; TEM, transmission electron microscopy.

Introduction

In all vertebrate organisms, G protein-coupled receptors (GPCRs) constitute a large superfamily of receptor proteins with similar overall topology responsible for signal transduction (see http://www.gpcr.org/7tm) [1,2]. In addition to communicating signals carried by fluctuating levels of hormones, neurotransmitters, and peptides across the plasma membrane, GPCRs mediate taste and odor recognition, as well as phototransduction in the retina. Three mammalian subfamilies of GPCRs have been identified (named A, B, and C), with family A being by far the largest (reviewed in refs. [1,3,4]). The members of the GPCR-A subfamily are more closely related to each other within a few functional regions than to the members of other subfamilies, although the overall sequence homology even within the subfamily is low.

GPCRs propagate their signals through the activation of their cognate G proteins and interactions with other signaling molecules [5,6]. The functional unit of these receptors in biosynthesis, resting state, and activation processes could not be identified due to the scarcity of these receptors in the native tissues and difficulties of working with membrane proteins. Yet, early work on these receptors provided strong evidence that GPCRs might operate as signaling dimers. For example, ligand binding assays suggested a cooperativity between adrenergic receptors [7]. Such cooperativity was likewise suggested by the observed modification of pharmacological properties of two co-expressed opioid receptor subtypes as compared to individually expressed subtypes [8]. Radiation inactivation studies pointed out the presence of oligomeric structures of GPCRs and G proteins [9]. A number of pharmacological and chemical methods were more recently employed to validate formation and function of oligomeric/dimeric forms of GPCRs, and insightful reviews were published [10–17]. These experimental results include direct functional and obligatory dimerization for the coupling and intracellular transport between two homologous subunits of γ-aminobutyric acid (GABA) receptors [18–20], dimeric structure of the extracellular domain of the metabotropic glutamate receptor, linked by a disulfide bridge [21], genetic and biochemical evidence of oligomerization of the α-factor receptor in yeast [22], Cys cross-linking indicating a symmetrical dimer interface in the dopamine D2 receptor [23], and identification of a pentameric complex between the dimeric leukotriene B4 receptor BLT1 and its G protein [24].

Retinal rod photoreceptors are post-mitotic neurons that are responsible for capturing visible photons and transducing the light signal via a biochemical cascade of reactions, which enable communication with the secondary neurons [25]. These events are initiated by conformational changes in the light-sensitive pigment, rhodopsin, which is one of the best studied GPCR. The light-induced conformational change of rhodopsin, known as bleaching, is followed by a series of second-messenger system reactions termed phototransduction [26,27]. Rods are highly differentiated cells with cylindrical outer segments (ROS) containing all components necessary for phototransduction. ROS are composed of stacks of 1000–2000 independent, pan cake-shaped disc membranes surrounded by a plasma membrane. The stacking of these internal cellular membrane structures ensures a dense packing of light-absorbing rhodopsins, which consti-

*To whom correspondence should be addressed.
e-mail: dimitrios.fotiadis@unibas.ch

Molecular Membrane Biology
ISSN 0968-7688 print/ISSN 1464-5203 online
http://www.tandf.co.uk/journals
DOI: 10.1080/09687860400020291

tute >90% of all disc membrane proteins, and in turn, a high probability of single photon absorption [28]. Rhodopsin occupies ≈50% of the space within the discs, corresponding to an approximately 3 mM concentration within ROS [29]. Knockout mice lacking rhodopsin do not develop ROS, indicating a structural role of rhodopsin in addition to its photon driven signaling function [30,31].

The high density of rhodopsin in disc membranes, the availability of native material, the high expression levels, and new biochemical and biophysical methods have all contributed to the leading role of studies on rhodopsin in the GPCR field (reviewed in ref. [32]). For example, the crystal structure of rhodopsin was recently elucidated [33], providing the first molecular details about how this GPCR binds its ligand, the chromophore 11-*cis*-retinal, and how it may activate the cognate G-proteins [27,34–37]. This structure also allowed construction and validation of numerous prediction models of other GPCRs (reviewed in ref. [38]). Recent biochemical studies demonstrated the existence of detergent-resistant membrane microdomains in ROS and therefore a non-uniform distribution of lipids and proteins [39–41]. In addition, the existence of rhodopsin dimers and higher oligomers organized into rafts and paracrystals has been demonstrated by transmission electron (TEM) and atomic force microscopy (AFM) in native murine disc membranes [42–44]. These data are further reinforced by a semi-empirical model of rhodopsin's supramolecular organization in the native membrane (model IV–V), and its interaction with transducin (a G protein) and arrestin (a regulatory protein) [43–46]. More recently, crosslinking experiments confirmed the existence of rhodopsin dimers [47]. A dimeric or higher oligomeric functional form of rhodopsin is supported by the structural information available on G proteins and rhodopsin, and biophysical data that identify different interacting regions on the interface between these proteins [48]. In particular, the size of the G protein surface interacting with rhodopsin has been shown to be almost twice as large as the exposed cytoplasmic surface of a single rhodopsin molecule [49,50].

However, all these results are in conflict with a model that assumes rapid diffusion of rhodopsin in the ''mosaic'' fluid disc membrane [51]. This view of the unobstructed mobility of the receptor was supported by biophysical measurements of rhodopsin diffusion and rotation in disc membranes, as well as by low-resolution neutron diffraction, mostly carried out in amphibian photoreceptors [52–55]. In most of these studies, photoactivation of rhodopsin did not affect the results (see also ref. [56]), suggesting that this lack of pre-organization did not change upon activation of rhodopsin.

In this work, we have used well-established and accessible methods to explore the higher order structure of rhodopsin in solution and in the native membrane. Bovine ROS membranes were prepared by the methods commonly employed by laboratories working on rhodopsin [57]. In contrast to our previous studies mainly by AFM, disc membranes were analyzed by TEM, blue native-polyacrylamide gel electrophoresis (BN-PAGE), sodium dodecyl sulphate-polyacrylamide gel electrophoresis (SDS-PAGE), chemical crosslinking, and by proteolysis. The results unequivocally point to the presence of rhodopsin dimers and higher oligomers in native bovine disc membranes.

Results

Transmission electron microscopy of isolated disc membranes

Negatively stained disc membranes from bovine ROS revealed the typical morphology for intact discs (Figure 1(*a*)). Power spectra (Figure 1(*b*)) calculated from circular disc membrane areas (broken circle 1) showed a diffuse ring at $\approx(45\ \text{Å})^{-1}$. This indicated paracrystallinity of rhodopsin in the native membrane as previously observed with disc membranes from mouse by TEM and AFM [42–44]. Power spectra calculated from circular carbon film regions (broken circle 2) did not reveal such diffuse diffraction (Figure 1(*c*)).

BN-PAGE of unbleached and bleached disc membranes

To explore the oligomeric state of rhodopsin in solution, DM-solubilized disc membranes were analyzed by BN-PAGE. Unbleached (Figure 2(*a*) and Figure 2(*b*); lane R) and bleached (Figure 2(*b*); lane O) samples revealed the

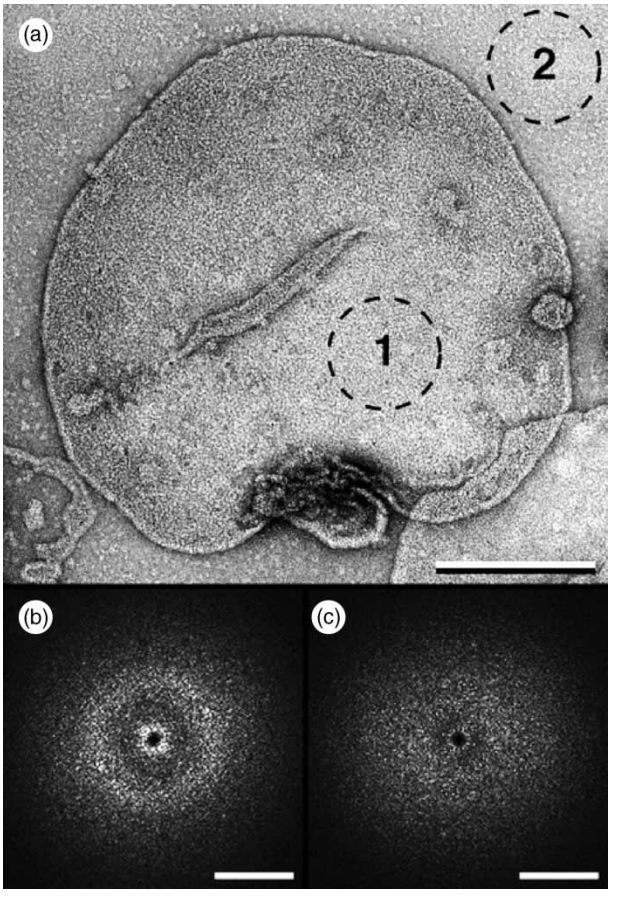

Figure 1. Transmission electron microscopy of negatively stained native disc membranes adsorbed on carbon film. (*a*) Morphology of a native disc membrane from bovine. (*b*) Average of five power spectra calculated from circular regions as marked on the displayed disc membrane by the broken circle (1). A diffuse powder diffraction signal is evident, indicating paracrystallinity of rhodopsin. (*c*) Average of five power spectra calculated from circular regions on the carbon film as marked by the broken circle (2). No powder diffraction is evident. Scale bars: 2000 Å (*a*) and $(40\ \text{Å})^{-1}$ (*b* and *c*).

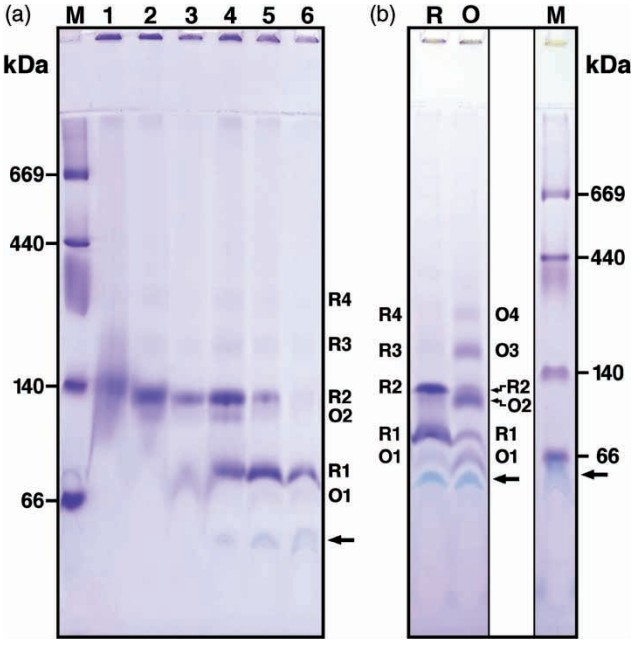

Figure 2. BN-PAGE of unbleached and bleached disc membranes. (*a*) Unbleached disc membranes solubilized in 0.3% (lanes 1–3) and 0.6% DM (lanes 4–6) at protein concentrations of ≈0.9 mg/ml (lane 1 and 4), ≈0.6 mg/ml (lane 2 and 5) and ≈0.3 mg/ml (lane 3 and 6). (*b*) Comparison between unbleached (lane R) and bleached (lane O) disc membranes. Both were solubilized in 0.6% DM at a protein concentration of ≈1.1 mg/ml. The BN-gels displayed in panels (*a*) and (*b*) are 5–12% linear gradient gels. Lanes labeled M: soluble markers thyroglobulin (669 kDa), ferritin (440 kDa), lactate dehydrogenase (140 kDa), and bovine serum albumin (66 kDa). Protein per lane: ≈18 μg (lanes 1, 4, R, and O), ≈12 μg (lane 2 and 5), and ≈6 μg (lane 3 and 6). This figure is reproduced in colour in *Molecular Membrane Biology* online.

presence of several protein bands on the non-denaturating gel. All visible bands were cut from the blue native-gel (BN-gel), the protein extracted from the gel and re-run by SDS-PAGE (data not shown). The latter confirmed the presence of only full-length rhodopsin/opsin in all bands (R1–R4 and O1–O4) except for the bright blue bands (see arrows). These bright blue bands did not indicate the presence of protein and were also detected in lanes containing only DM or in the marker upon addition of DM (see Figure 2(*b*); lane M, arrow). The calculated apparent masses (M_{app}) of the different rhodopsin and opsin bands are listed in Table 1.

Figure 2(*a*) displays unbleached disc membranes, which were solubilized in 0.3% (lanes 1–3) or 0.6% DM (lanes 4–6) at protein concentrations of ≈0.9 mg/ml (lane 1 and 4), ≈0.6 mg/ml (lane 2 and 5), and ≈0.3 mg/ml (lane 3 and 6). Two prominent bands were detected in the BN-gel, one at ≈85 kDa (R1 in Figure 2(*a*)) and one at ≈125 kDa (R2 in Figure 2(*a*)). Using the conversion factor given by Heuberger *et al*. (2002) [58] to estimate the mass of membrane proteins on BN-gels, we assigned the R1 and R2 bands to the rhodopsin monomer and dimer (see Table 1). A dimer to monomer transition was observed at decreasing protein but constant DM concentrations (see lanes 1–3 and 4–6). This detergent-induced dissociation of rhodopsin dimers into monomers was more striking at the higher DM concentration, as illustrated in Figure 2(*a*), which compares the disc membranes solubilized in 0.3% DM (lanes 1–3) with the membranes solubilized in 0.6% DM (lanes 4–6). Under certain experimental conditions, rhodopsin dimers (Figure 2(*a*); R2 in lane 2) or monomers (Figure 2(*a*); R1 in lane 6) were found almost exclusively. Similar detergent-induced dissociation of rhodopsin dimers were also observed in BN-gels of Triton X-100 or CYMAL®-7 solubilized disc membranes (data not shown).

Besides the prominent bands R1 and R2, weak bands labeled O1, O2, R3, and R4 migrating at ≈65 kDa, ≈110 kDa, ≈175 kDa, and ≈245 kDa were also seen. A similar dissociation effect as observed for R1 and R2 was also found for O1 and O2. The intensity of O2 decreased while that of O1 increased upon decreasing the protein concentration at constant DM concentration (lanes 4–6 in Figure 2(*a*)). Significant differences in the intensities of the single protein bands were found between unbleached (Figure 2(*a*) and 2(*b*); lane R) and bleached disc membranes (Figure 2*(b*); lane O). While the bands at ≈65 kDa, ≈110 kDa, ≈175 kDa, and ≈245 kDa in BN-gels of unbleached disc membranes were weak, these bands were prominent in BN-gels of bleached disc membranes. On the other hand, the prominent bands at ≈85 kDa and ≈125 kDa on BN-gels of unbleached disc membranes were weak in BN-gels of bleached disc membranes.

Transmission electron microscopy of DM-solubilized disc membranes

When disc membranes were solubilized under conditions that preserved the dimeric state of rhodopsin in BN-PAGE experiments and prepared by negative staining for TEM analysis (see experimental procedures), a homogeneous particle distribution was observed (Figure 3). Bi-lobed roughly conical structures with a length of 65 ± 6 Å ($n = 55$) and a separation of the density maxima of 32 ± 4 Å ($n = 53$) represented the majority of the particles. Their morphology and dimensions are compatible with those of rhodopsin dimers viewed side-on.

Table 1. Apparent and detergent-free masses of protein bands detected by BN-PAGE.

Protein band label	R1	R2	R3	R4	O1	O2	O3	O4
M_{app} (in kDa)*	≈85	≈125	≈175	≈245	≈65	≈110	≈175	≈245
M_{df} (in kDa)**	≈45	≈70	≈95	≈135	≈35	≈60	≈95	≈135

*The apparent mass (M_{app}) was estimated according to the soluble marker proteins.
**The detergent-free mass (M_{df}) was estimated according to Heuberger *et al.* (2002) [58].

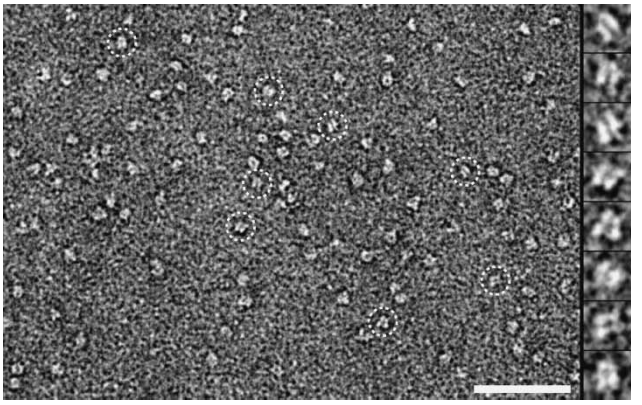

Figure 3. Transmission electron microscopy of negatively stained DM-solubilized disc membranes. Rhodopsin dimers are clearly discerned on the carbon film. The selected particles which are marked by broken circles were magnified and are displayed in the gallery. The scale bar represents 500 Å. The frame size of the magnified particles in the gallery is 104 Å.

Chemical crosslinking of disc membranes with DSP

In an attempt to unveil the interacting domains in the rhodopsin oligomer, isolated native disc membranes were crosslinked with the amino-specific homobifunctional N-hydroxysuccinimide ester and thiolcleavable crosslinker DSP. Disc membranes (protein concentration: 100 μg/ml) were treated with different concentrations of DSP (0, 0.5, 1, 2.5, and 5 mM) for 15 h and run by SDS-PAGE in the absence (Figure 4(*a*)) and in the presence (Figure 4(*b*)) of 2-mercaptoethanol (2-ME; final concentration: 3%) in the sample-buffer (SB). In the former, a clear formation of rhodopsin dimers (band between the 75 and 100 kDa marker) and higher oligomers was observed (bands above the 100 kDa marker), as well as a continuous decrease of the monomer band intensity (band below the 37 kDa marker) at increasing DSP concentrations. Upon addition of 2-ME the majority of the chemically coupled rhodopsin oligomers migrated as monomers, leaving only weak dimer bands (Figure 4(*b*)) and indicating successful crosslinking by DSP. In a second experiment, the kinetics of the crosslinking process at 2.5 mM DSP were explored, showing an increase in rhodopsin dimers and oligoforms and a decrease in rhodopsin monomer bands when the incubation time was increased (Figure 4(*c*)). The majority of the crosslink products were cleaved by 2-ME containing SB (Figure 4(*d*)). In a third experiment, the dependence of the protein concentration at 2.5 mM DSP for 15 h was investigated (Figure 4(*e*)). Halving or doubling the protein concentration used in the experiments described in Figures 4(*a*)–4(*d*), i.e., 100 μg/ml, did not influence the high efficiency of the crosslinker. DSP crosslink products were again cleaved by the addition of 2-ME to the SB (Figure 4(*f*)).

To localize the sites of modification by DSP, crosslinked rhodopsin was cleaved with thermolysin while still in the disc membrane. The sites of cleavage are well documented [59,60]: thermolysin cleaves rhodopsin at the loop region between helices H–V and H–VI into two pieces. The large N-terminal fragment (≈26 kDa) containing residues 1–240 is termed F1, and the short fragment (≈13 kDa) containing residues 241–327 is termed F2. In addition, thermolysin cleavage also generates three small fragments from the C-terminal end that are released into the supernatant. Thermolysin treatment of crosslinked disc membranes and subsequent analysis by SDS-PAGE revealed the monomeric and dimeric forms of rhodopsin as well as the F1 fragment (Figure 4(*g*)). SDS-PAGE of the same sample but after incubation in SB containing 2-ME resulted in (i) large amounts of F1 and F2 rhodopsin fragments (Figure 4(*h*); bands F1 and F2), (ii) a drastic decrease in rhodopsin dimers and higher oligomers, and (iii) two residual populations of monomers with different lengths of the C-termini (Figure 4(*h*); bands m). This result strongly indicates crosslinking between F1 and F2 fragments of rhodopsin. To further substantiate these observations, the monomeric and dimeric rhodopsin bands in Figure 4(*g*) (bands m and d) were cut from the SDS/polyacrylamide gel, the protein extracted from the gel piece, and the extract re-run by SDS-PAGE; see Figure 4(*i*), left lane: extract from the monomer band, right lane: extract from the dimer band (no 2-ME in the SB). Figure 4(*j*) shows the same experiment as in Figure 4(*i*), but after incubation of the samples with 2-ME containing SB. For the extracted monomer band, cleavage of the crosslinker by 2-ME identified crosslinking of F1 with F2 (Figure 4(*j*); left lane). Valuable information on the rhodopsin domains crosslinked by DSP and therefore interacting in the oligomer were obtained from the overexposed silver-stained SDS/polyacrylamide gel of the extracted dimer band (Figure 4(*j*); right lane). Incomplete cleavage of the crosslinker by 2-ME yielded the two bands below the dimer band (band d in Figure 4(*j*); right lane). These two bands with apparent masses of ≈49 kDa and ≈57 kDa were attributed to crosslink products between the fragments $F2^{Rho1}$-$F1^{Rho1}$-$F2^{Rho2}$ and $F1^{Rho1}$-$F2^{Rho2}$-$F1^{Rho2}$ of two rhodopsin molecules.

Chemical crosslinking of disc membranes with LC-SPDP

As an alternative to the amino-specific crosslinker DSP, the thiol-specific heterobifunctional N-hydroxysuccinimide ester-pyridyldithiol and thiolcleavable crosslinker LC-SPDP was used to treat native disc membranes. Membrane preparations (protein concentration: 100 μg/ml) were incubated at different concentrations of LC-SPDP (0, 25, 100, and 250 μM) for 15 h and run by SDS-PAGE in the absence (Figure 5(*a*)) and in the presence (Figure 5(*b*)) of 2-ME (final concentration: 3%) in the SB. In the former, formation of rhodopsin dimers was evident, but at much lower amounts compared to DSP: this is the result of low solubility of LC-SPDP which allowed only concentrations up to 250 μM to be tested. Upon addition of 2-ME the majority of the chemically coupled rhodopsin dimers returned to the monomeric state (Figure 5(*b*)), indicating successful crosslinking by LC-SPDP. In a second experiment, kinetics of the crosslinking process at 250 μM LC-SPDP were explored, showing an increase in the amount of rhodopsin dimer as a function of the incubation time (Figure 5(*c*)). Again, the majority of the crosslink products were cleaved by 2-ME containing SB (Figure 5(*d*)). Similar to the experiments with DSP, rhodop-

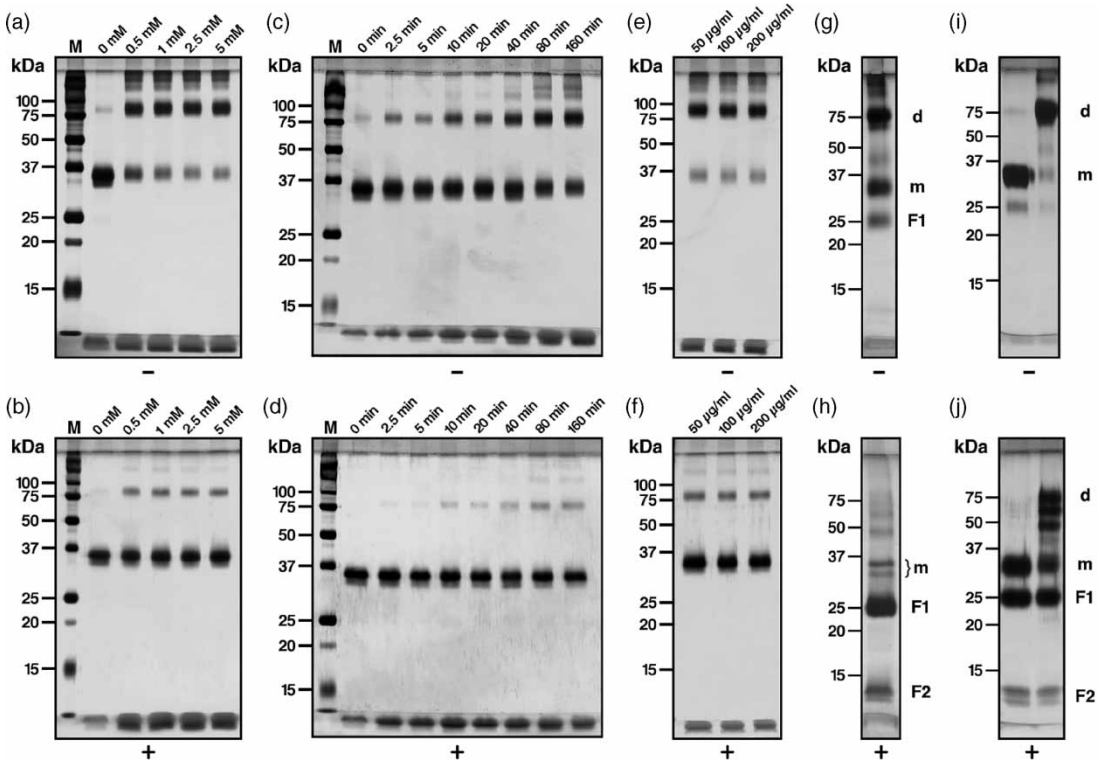

Figure 4. SDS-PAGE of bovine disc membranes crosslinked in the presence of DSP. (*a*) Crosslinking of isolated disc membranes at different concentrations of DSP. Incubation for 15 h at 4°C. No 2-ME in the SB. (*b*) Same as (*a*) but with 2-ME in the SB. (*c*) Time course of crosslinking at 2.5 mM DSP. No 2-ME in the SB. (*d*) Same as (*c*) but with 2-ME in the SB. Protein concentration during the crosslinking reactions in (*a*–*d*): 100 µg/ml. (*e*) Crosslinking at 2.5 mM DSP and different disc membrane protein concentrations (50, 100 and 200 µg/ml). No 2-ME in the SB. (*f*) Same as (*e*) but with 2-ME in the SB. (*g*) Disc membranes crosslinked in the presence of 2.5 mM DSP and subsequently digested with thermolysin. Incubation for 15 h at 4°C for both, crosslinking and protease treatment, respectively. No 2-ME in the SB. (*h*) Same as (*g*) but with 2-ME in the SB. (*i*) Crosslinked and thermolysin-digested rhodopsin monomers (m; left lane) and dimers (d; right lane) after extraction from gels such as that displayed in panel (*g*). No 2-ME in the SB. (*j*) Same as (*i*) but with 2-ME in the SB. Band labels: m, rhodopsin monomer; d, rhodopsin dimer; F1 and F2, proteolytic fragments of rhodopsin after thermolysin digestion. The 13.5% SDS-polyacrylamide gels (*a*–*j*) are silver-stained. '+' means sample was mixed with SB containing 2-ME (final concentration: 3% 2-ME) and '−' means sample was mixed with SB without 2-ME.

sin was cleaved by thermolysin to localize the sites modified by LC-SPDP. Protease treatment of crosslinked disc membranes and subsequent analysis by SDS-PAGE produced the gel displayed in Figure 5(*e*). Significant amounts of two monomer species with differing length of their C-termini and F1 fragments as well as low amounts of F2 fragments were detected. The distinct dimer band (see Figure 5(*a*) and (*c*)) is distributed over a series of weak bands between the 100 kDa and the 37 kDa marker (Figure 5(*e*)). SDS-PAGE of the same sample after incubation in SB containing 2-ME revealed a decrease in the quantity of monomeric rhodopsin and a significant increase of F1 and F2 fragments (Figure 5(*f*)). This result indicates successful crosslinking of the F1 and F2 rhodopsin fragments by LC-SPDP.

Discussion

Transmission electron microscopy of isolated disc membranes

A wealth of low-resolution structural information on membrane proteins has been acquired by electron microscopy of negatively stained preparations [61]. We have used this efficient and well-established approach to characterize disc membranes prepared at room temperature from wild-type and transgenic mice [43,62]. They all revealed the characteristic diffuse diffraction ring at $\approx(45\ \text{Å})^{-1}$ observed in this study for bovine disc membranes. Therefore, the supramolecular arrangement of bovine rhodopsin in the discs is highly similar to that of murine rhodopsin and was unaffected by the freezing of ROS and the storage of isolated disc membranes at 4°C. Taken together, these results also document that the power spectra of images from negatively stained native disc membranes efficiently unveil paracrystalline structures that are barely discernable by naked eye on electron micrographs.

BN-PAGE of unbleached and bleached disc membranes

BN-PAGE introduced by Schägger and von Jagow (1991) [63] is an attractive method to characterize the oligomeric state of proteins under close-to-native conditions. The results summarized in Figure 2 strongly suggest that the major fraction of native rhodopsin exists as a dimer. However, they

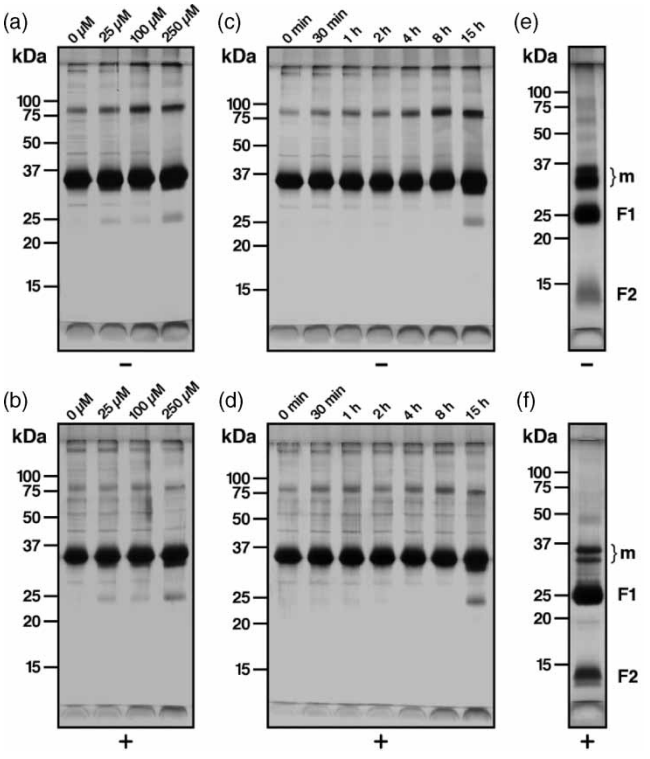

Figure 5. SDS-PAGE of bovine disc membranes crosslinked in the presence of LC-SPDP. (*a*) Crosslinking of isolated disc membranes at different concentrations of LC-SPDP. Incubation for 15 h at 4°C. No 2-ME in SB. (*b*) Same as (*a*) but with 2-ME in the SB. (*c*) Time course of crosslinking at 250 μM LC-SPDP. No 2-ME in the SB. (*d*) Same as (*c*) but with 2-ME in the SB. Protein concentration during the crosslinking reactions in (*a*–*d*): 100 μg/ml. (*e*) Disc membranes crosslinked in the presence of 250 μM LC-SPDP and subsequently digested with thermolysin. Incubation for 15 h at 4°C for crosslinking and protease treatment, respectively. No 2-ME in the SB. (*f*) Same as (*e*) but with 2-ME in the SB. Band labels: m, rhodopsin monomer; F1 and F2, proteolytic fragments of rhodopsin after thermolysin digestion. The 13.5% SDS-polyacrylamide gels (*a*–*f*) are silver-stained. '+' means sample was mixed with SB containing 2-ME (final concentration: 3% 2-ME) and '−' means sample was mixed with SB without 2-ME.

also illustrate that BN-PAGE requires careful adjustment of experimental conditions to obtain meaningful results (related to this topic: see ref. [58]). In the case of rhodopsin, the ratio of detergent-to-protein concentrations and the amount of bound Coomassie brilliant blue G-250 (CCB) are critical factors, similar to experiments with the lactose transporter LacS [58]. The DM-dependent dissociation of the rhodopsin dimer detected by BN-PAGE was not specific to DM but was also observed for other detergents, i.e. Triton X-100 and CYMAL®-7. These results are further supported by the disruption of the oligomeric state of the dopamine D2 receptor upon membrane solubilization with 0.5% DM [23] and by the detection of almost exclusively dimers and higher oligomers of the latter in native, non-denaturating gels [64]. Another indication for the fragility of the native rhodopsin dimer is found in rhodopsin's crystal structure [33]. In 3D crystals, rhodopsin is seen to pack as a monomeric unit when solubilized with the harsh (compared to DM) short alkyl chain detergent nonyl-β-D-glucoside [65].

In spite of working in the dark or under dim red light, a small fraction of opsin was present in unbleached membranes. On the other hand, a small fraction of rhodopsin was present after bleaching the membranes, allowing identification of rhodopsin (R) and opsin (O) as bands with different mobilities on the BN-gel (Figure 2). Both species exhibited a similar behavior, although opsin had a stronger propensity to form oligomers, i.e. trimers and tetramers than rhodopsin. This property of opsin is likely the result of a light-induced conformational change and may be explained as unspecific aggregation of opsin through sticky domains, e.g. the recently identified hydrophobic patch in the cytoplasmic face of rhodopsin exposed during receptor activation [66]. In addition, based on the recent results from TEM and AFM on the oligomeric state of rhodopsin and opsin in native membranes [44], the opsin oligomers seen in BN-gels may also be interpreted as a stronger light-induced interaction between opsin than between rhodopsin molecules in rafts and paracrystals. Finally, the bright blue bands (arrows in Figure 2) which stained differently compared to R1–R4 and O1–O4 and did not indicate the presence of protein were attributed to DM/CCB micelles.

Transmission electron microscopy of DM-solubilized disc membranes

Negative stain TEM of bovine disc membranes solubilized with DM under conditions that warrant a major fraction of rhodopsin dimers by BN-PAGE revealed bi-lobed particles (Figure 3). The particle dimensions are compatible with those expected for rhodopsin dimers (see ref. [35] for the dimensions of rhodopsin). These results from TEM also exclude a possible CCB induced oligomerization of rhodopsin during BN-PAGE since no CCB was present during sample preparation for TEM (see experimental procedures). In summary, the results from these two independent methods, i.e. TEM and BN-PAGE, strongly suggest the dimers observed to represent the native oligomeric state of rhodopsin.

Chemical crosslinking of rhodopsin in native disc membranes

Only two reports on crosslinking of rhodopsin in native disc membranes have been published in the last few decades [47,67]. In the work by Downer (1985) [67], the observed crosslinking of rhodopsin by glutaraldehyde was interpreted as crosslinking upon random collision between diffusing rhodopsin monomers in the disc membrane. This interpretation was based on the kinetics of glutaraldehyde crosslinking. However, considering the complexity of possible glutaraldehyde reaction mechanisms, in particular its tendency to form highly reactive polymers (e.g. α, β,-unsaturated aldehyde) of different chain lengths [68] it is difficult to interpret these results conclusively. Specific crosslinkers were used in the very recent work by Medina *et al.* (2004) [47] who detected rhodopsin dimers and higher oligomers. In contrast to Downer [67], Medina *et al*. have interpreted the observed rhodopsin crosslink products as a result of the native oligomeric assembly of rhodopsin and not as crosslink

between random collision complexes of monomeric rodopsin molecules.

In the present work, the crosslinkers DSP and LC-SPDP were selected according to their chemical and structural properties and their spacer lengths according to the distances between reactive Lys and Cys residues on the cytoplasmic surface of the current rhodopsin oligomer model IV–V (Figure 6; Protein Data Bank accession number 1N3M [43–45]). Crosslinkers containing the thiol-reactive maleimide group were not considered, because of the unspecific reactions with Lys residues [69]. Instead, crosslinkers containing the sulfhydryl-specific pyridyl disulfide group were employed, i.e. LC-SPDP. DSP and LC-SPDP were also selected because of their cleavability by reducing agents, allowing control experiments as those presented in Figures 4 and 5 to be performed.

DSP and LC-SPDP crosslinking with subsequent SDS-PAGE analyses clearly demonstrated the chemical trapping of rhodopsin dimers and higher oligomers, and therefore their existence in the native disc membrane. Among the two reagents used, DSP was more effective than LC-SPDP, which is plausible considering the low solubility of LC-SPDP and the numerous Lys residues compared to the few Cys residues at the cytoplasmic surface of rhodopsin [60]. Thermolysin treatment of DSP or LC-SPDP crosslinked disc membranes yielded a small set of well-defined rhodopsin fragments and not a large set of species as expected for random crosslinks between proteolytic fragments (Figures 4 and 5). The former together with the results from TEM (Figure 1) and AFM [42–44] strongly suggests specific crosslinking between rhodopsin molecules organized in a higher order structure rather than crosslinking by random collisions of freely-diffusible rhodopsin molecules as previously suggested by Downer [67]. The defined proteolytic rhodopsin fragments also indicated that thermolysin could not access the intradiscal space excluding therefore an opening of the disc membranes by the used low concentrations of DMSO and DMF during crosslinking. After thermolysin treatment of crosslinked disc membranes, two populations of rhodopsin monomers were seen as double bands (see Figures 4 and 5; band m): this was attributed to monomers with uncleaved and cleaved C-termini, which is supported by the observation that the first part of rhodopsin being attacked by proteases was the carboxyl terminus [60].

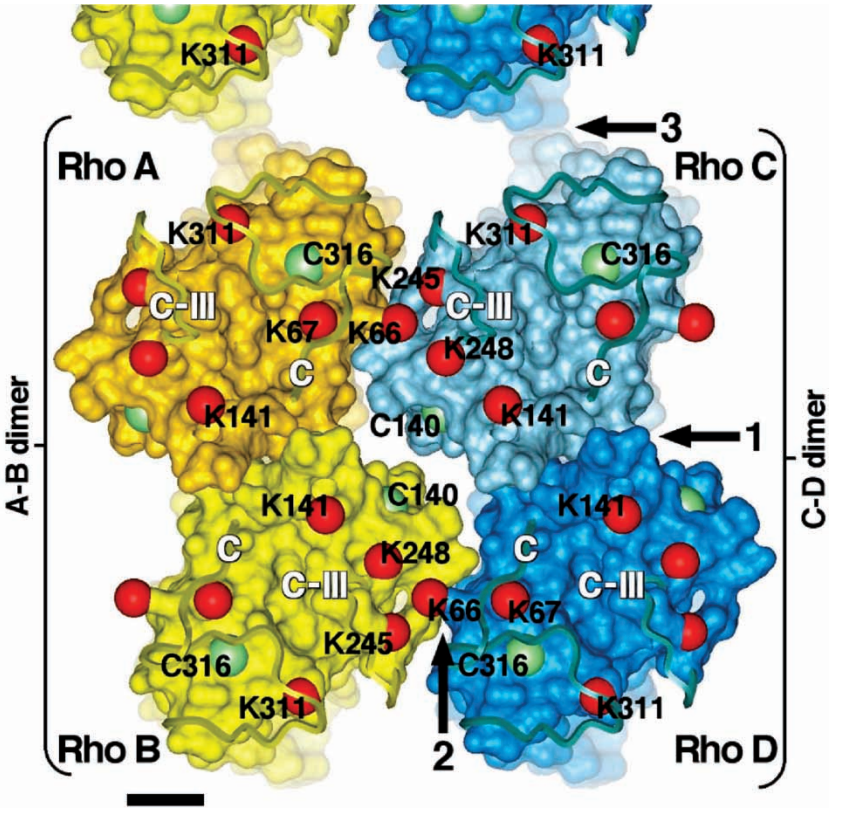

Figure 6. Location of selected Lys and Cys residues on the cytoplamic surface of the molecular model of the rhodopsin oligomer (model IV–V). Red balls indicate the reactive Lys ε-amino groups while the green balls indicate the reactive β-thiol groups of the Cys residues. Distances between selected groups are summarized in Table 2. The intra- (contact 1) and interdimeric contacts (contact 2) as well as the row–row contacts (contact 3) forming the higher-order structure of rhodopsin are indicated. For better clarity, the C-termini (labeled c) as well as parts of the C-III loops (labeled C-III) are displayed as wires and the one letter instead of the three letter code was used for the highlighted amino acid residues. Unlabelled balls can be assigned by symmetry. The coordinates of model IV–V are deposited at the Protein Data Bank (accession code 1N3M) [42–44]. The scale bar represents 10 Å.

Intra- and intermolecular crosslinking of rhodopsin according to model IV–V

The semi-empirical model of the active rhodopsin dimer deposited in the protein data base (access code 1N3M) has been established based on the packing arrangement of rhodopsin in the native murine disk membrane [43,44]. This model and its implication for the interaction of rhodopsin with its regulator, arrestin, and its cognate G-protein, transducin, have been extensively discussed recently [45]. Here, the model is used to interpret the crosslinking and thermolysin digestion experiments.

Nine Lys residues exposed on the cytoplasmic surface of bovine rhodopsin to the solvent could react with the amino-specific homo-bifunctional crosslinker DSP: Lys-66, Lys-67, Lys-141, Lys-231, Lys-245, Lys-248, Lys-311, Lys-325, and Lys-339 (Figure 6). According to the labeling study by Barclay and Findlay (1984) [70] all of them react strongly with hydrophilic chemical probes with the exception of Lys-231 on the third cytoplasmic loop, and Lys-325, which is only weakly reactive. Since Lys-339 is located at the thermolysin-cleaved C-terminus of rhodopsin [60,71], only six lysines have the capacity to covalently stabilize the dimer, maintaining its conformation after thermolysin treatment. Thus, the Lys residues of interest are: Lys-66, Lys-67, Lys-141, Lys-245, Lys-248, and Lys-311. The related distances between accessible Lys residues less than 20 Å apart, determined according to the dimer model (Figure 6), are listed in Table 2. The corresponding possible crosslink products and their proteolytic fragments are given in Table 3. Accordingly, the crosslinked, thermolysin-cleaved rhodopsin dimer, which migrates at $\approx$75 kDa (Figure 4(*i*)) due to the loss of the C-terminus, is expected to dissociate after incomplete reduction into the following species: a monomer crosslinked with one F1 ($\approx$57 kDa), a monomer crosslinked with one F2 ($\approx$49 kDa), the monomer, fragment F1, and fragment F2, exactly as revealed by Figure 4(*j*).

Among the ten Cys residues of bovine rhodopsin, only Cys-140 and Cys-316 can react with thiol-specific reagents. Other cysteine residues are intradiscal (Cys-110, Cys-185, and Cys-187 [33]), are palmitoylated (Cys-322 and Cys-323 [72]), or are buried within the transmembrane helices (Cys-167, Cys-222, and Cys-264 [33]). Numerous studies with thiol-reactive reagents have shown that Cys-316 is significantly more reactive than Cys-140 [71,73–76]. Therefore, we have used the heterobifunctional, thiol-specific crosslinker LC-SPDP. The distances between either Cys-316 or Cys-140 and accessible Lys residues less than 20 Å away, determined according to the dimer model (Figure 6), are listed in Table 2 as well. Accordingly, intermolecular crosslinks can only be obtained by the slow reaction of LC-SPDP with Cys-140 and Lys-66 that is within the range of the LC-SPDP spacer length. This and the low solubility of LC-SPDP fully explain the small amount of rhodopsin dimers stabilized by this reagent (Figure 5(*a*) and (*c*)). On the other hand, LC-SPDP can efficiently crosslink the fast-reacting Cys-316 with either Lys-66 or Lys-67 of the same rhodopsin molecule, which explains the preservation of rhodopsin monomers during thermolysin-treatment (Figure 5(*e*)). Most of this monomeric fraction dissociates into fragments F1 and F2 when submitted to reducing conditions, demonstrating strong intramolecular crosslinking (Figure 5(*f*)). In addition, thermolysine digestion leads to a ladder of weak bands that migrate between the 100 kDa and 37 kDa markers (see Figure 5(*e*)) under non-reducing conditions. They correspond to the crosslinked proteolytic products predicted from model IV–V, which are listed in Table 3.

Taken together, the crosslinking experiments clearly document the existence of highly specific rhodopsin dimers. In addition, the rhodopsin dimer model IV–V allows all the possible crosslinks with both types of reagents and the corresponding thermolysin-induced fragments to be predicted. All the experimental data shown in Figures 4 and 5 are fully compatible with these predictions.

We have demonstrated by structural and biochemical methods that bovine rhodopsin consists mainly of dimers and higher oligomers in native membranes. These observations are in line with our previous results from TEM and AFM using native disc membranes from mouse. Furthermore, the results from crosslinking with DSP and LC-SPDP support our present model IV–V of the rhodopsin dimer/oligomer [43–45]. The spatial resolution provided by the crosslinking experiments does not suffice to fully verify the correctness of this semi-empirical model, but they strongly restrain the possible configurations. High-resolution structural information is now required to confirm the proposed conformation of the rhodopsin dimer and its interaction with the G-protein heterotrimer.

Experimental procedures

Chemicals

The homobifunctional crosslinker dithiobis(succinimidyl propionate) (DSP; extended linear spacer length: 12 Å) and the heterobifunctional crosslinker succinimidyl-6-[3-(2-pyridyldithio)-propionamido]hexanoate (LC-SPDP; extended linear spacer length: 15.7 Å) were purchased from Pierce (Perbio Science, Switzerland). The detergents n-dodecyl-β-D-maltoside (DM) and 7-cyclohexyl-1-heptyl-β-D-maltoside (CYMAL®-7) were obtained from Anatrace (Maumee, OH, USA) and Triton X-100 from Sigma (Switzerland).

Preparation of ROS and isolation of disc membranes

Bovine ROS were prepared from fresh retinas according to Papermaster [57] and stored at −80°C in 67 mM potassium phosphate (pH 7.0), 1 mM magnesium di(acetate), 0.1 mM EDTA, 1 mM dithiothreitol (DTT), until further use. An aliquot of 3 ml ROS at protein concentrations between 12–15 mg/ml was split into four centrifuge tubes, filled up to 1 ml with cold water and centrifuged (110,000*g* at r_{av}; 15 min; 4°C). The supernatants were discarded, the tubes refilled to 1 ml with cold water, the pellet resuspended and centrifuged. This procedure was repeated one more time with cold water and twice with a 300 mM NaCl solution. Finally, the pellets containing the disc membranes were pooled and diluted with 300 mM NaCl to a final concentration of 5.67 mg/ml or 6.67 mg/ml protein, depending on the experiment. Samples were always kept at 4°C in the dark and manipulations were performed under dim red light (Ilford Iso 906 filter).

TEM and image processing of negatively stained samples

Isolated discs or DM-solubilized disc membranes were adsorbed to glow discharged carbon support films mounted on electron microscopy grids and negatively stained with 2% uranyl acetate or 0.75%

Table 2. Inter- and intramolecular distances <20 Å in model IV–V*.

(a) Intermolecular distances between Lys residues at the dimer-dimer interface.

Lys residues:	Distances from Lys ε-amino groups:
Lys-66A – Lys-245C	6.7 Å**
Lys-66A – Lys-248C	7.7 Å**
Lys-67A – Lys-245C	16.6 Å
Lys-67A – Lys-248C	17.9 Å

(b) Intramolecular distances between Lys residues on F1 and F2 fragments.

Lys residues:	Distances from Lys ε-amino groups:
Lys-141 (F1) – Lys-248 (F2)	10.2 Å**
Lys-67 (F1) – Lys-311 (F2)	17.2 Å
Lys-141 (F1) – Lys-245 (F2)	17.5 Å

(c) Intermolecular distances between Cys-140 and Lys residues at the dimer-dimer interface.

Amino acid residues:	Distances from Lys ε-amino groups to Cys β-thiol groups
Cys-140C – Lys-66A	14.2 Å**

(d) Intramolecular distances between Cys-316 and Lys residues on F1.

Amino acid residues:	Distances from Lys ε-amino groups to Cys β-thiol groups
Cys-316 (F2) – Lys-67 (F1)	9.8 Å**
Cys-316 (F2) – Lys-66 (F1)	14.3 Å**

*The atomic coordinates and structure factors of model IV–V [43,44] (code 1N3M) are deposited in the Protein Data Bank (http://www.rcsb.org/).
**Possible crosslinking partners based on the spacer lengths of DSP (12 Å) and LC-SPDP (15.7 Å). Intermolecular distances of the symmetry related B–D dimer (Figure 6) are not listed.

uranyl formate, respectively. To achieve a homogeneous particle distribution, disc membranes (protein concentration: 0.3 mg/ml) were solubilized in 0.3% DM, diluted 100-fold in 20 mM Tris-HCl (pH 7.7), 150 mM NaCl, 0.01% NaN_3, 0.04% DM and adsorbed on glow discharged TEM grids. Electron micrographs were recorded with a Hitachi H-7000 electron microscope operated at 100 kV. Single power spectra of electron micrographs and averages of several power spectra were calculated with the SEMPER image processing system [77].

Electrophoretical and analytical methods

Linear 5–12% gradient gels for BN-PAGE were prepared and run as previously described by Schägger and von Jagow (1991) [63], but in the dark. Prior to BN-PAGE, an aliquot of disc membranes was bleached three times by a photographic flashlight from 5 cm distance. Both, bleached and unbleached disc membranes were then solubilized in 0.3% or 0.6% DM (30 min at 4°C in the dark) and run by BN-PAGE. Samples for SDS-PAGE were run on 13.5% SDS/polyacrylamide gels and silver-stained. Protein concentrations were determined using the BCA assay (Pierce).

Chemical crosslinking of disc membranes with DSP

Crosslink reactions of disc membranes with DSP were performed at pH 8 in 20 mM HEPES-NaOH, 300 mM NaCl. DSP was solubilized in dimethly sulfoxide (DMSO) to a concentration of 100 mM (stock solution). Crosslinking was initiated by the addition of the corresponding volume of DSP stock solution to the disc membranes. All crosslinking trials including the negative controls (no DSP) contained 5% DMSO. The protein and DSP concentrations as well as further experimental details, e.g. incubation times, are indicated in the results section and in the legend to Figure 4. Crosslink reactions were terminated by the addition of glycine from a 1 M stock solution to a final concentration of ≈48 mM. The crosslinked and control membranes were subsequently washed three times by centrifugation (16,000*g* at r_{av}; 15 min; 4°C) with 20 mM HEPES-NaOH (pH 7.6), 300 mM NaCl. Samples were always kept at 4°C in the dark and manipulations were performed under dim red light.

Chemical crosslinking of disc membranes with LC-SPDP

Crosslink reactions with LC-SPDP were performed at pH 7 in phosphate buffered saline (PBS). LC-SPDP was solubilized in N,N′-dimethylformamide (DMF) to a concentration of 10 mM (stock

Table 3. Possible thermolysin fragments of crosslinked rhodopsin dimers according to model IV–V*.

Fragment species	Calculated molecular mass$^+$	Crosslinks	Reagent
$F2^{RhoA}$-$F1^{RhoA}$-$F2^{RhoC}$	52 kDa	Lys-141A – Lys-248A and Lys-66A – Lys-245C	DSP
$F1^{RhoA}$-$F2^{RhoC}$-$F1^{RhoC}$	65 kDa	Lys-66A – Lys-245C and Lys-141C – Lys-248C	DSP
$F1^{RhoA}$-$F1^{RhoC}$	52 kDa	Cys-140C – Lys-66A	LC-SPDP
$F1^{RhoA}$-$F1^{RhoC}$-$F2^{RhoC}$	65 kDa	Cys-140C – Lys-66A and Cys-316C – Lys-67C	LC-SPDP

*The atomic coordinates and structure factors of model IV–V [43,44] (code 1N3M) are deposited in the Protein Data Bank (http://www.rcsb.org/).
$^+$When comparing the calculated molecular masses with the apparent masses of the bands in Figure 4(*j*) (right lane), the loss of the C-terminus resulting from thermolysin cleavage should be considered.
Intermolecular distances of the symmetry related B–D dimer (Figure 6) are not listed.

solution). Crosslinking was initiated by the addition of the corresponding volume of LC-SPDP stock solution to the disc membranes. All crosslinking trials, including the negative controls (no LC-SPDP), contained 2.5% DMF. The protein and LC-SPDP concentrations as well as further experimental details such as incubation times, are indicated in the results section and in the legend to Figure 5. Crosslink reactions were terminated by the addition of a 100 mM glycine and 100 mM DTT mixture to a final concentration of 1 mM glycine and DTT. The crosslinked and control membranes were subsequently washed three times by centrifugation (16,000*g* at r_{av}; 15 min; 4°C) with 20 mM HEPES-NaOH (pH 7.6), 300 mM NaCl, 1 mM DTT, 1 mM glycine. Samples were always kept at 4°C in the dark and manipulations were performed under dim red light.

Thermolysin digestion of crosslinked disc membranes

The DSP or LC-SPDP crosslinked disc membranes (≈25 μg protein) were suspended in 50 μl of 20 mM HEPES-NaOH (pH 7.6), 300 mM NaCl containing 5 mM $CaCl_2$ and 3 mg/ml thermolysin (Sigma). After digestion (15 h; 4°C) membranes were washed three times by centrifugation (16,000*g* at r_{av}; 15 min; 4°C) in 20 mM HEPES-NaOH (pH 7.6), 300 mM NaCl. Samples were always kept at 4°C in the dark and manipulations were performed under dim red light.

Acknowledgements

A.E. and D.F. acknowledge support by the Swiss National Research Foundation, the M. E. Müller Foundation, the Swiss National Center of Competence in Research (NCCR) 'Structural Biology' and the NCCR 'Nanoscale Science'. S.F. acknowledges the support by the Polish State Committee for Scientific Research (grant 3P05F02625). K.P. was supported by a NIH grant EY09339, a grant from Research to Prevent Blindness, Inc. (RPB) to the Department of Ophthalmology at the University of Washington, the Stargardt and Retinal Eye Disease Fund, and a grant from the E.K. Bishop Foundation. The authors are indebted to Dr Paul Park for his comments on the manuscript and to Dr Paul Werten for the inspiring discussions.

References

[1] Gether, U., 2000, Uncovering molecular mechanisms involved in activation of G protein-coupled receptors. *Endocr. Rev.*, **21**, 90–113.
[2] Mirzadegan, T., Benko, G., Filipek, S. and Palczewski, K., 2003, Sequence analyses of G-protein-coupled receptors: similarities to rhodopsin. *Biochemistry*, **42**, 2759–2767.
[3] Ballesteros, J. and Palczewski, K., 2001, G protein-coupled receptor drug discovery: implications from the crystal structure of rhodopsin. *Curr. Opin. Drug Discov. Devel.*, **4**, 561–574.
[4] Ballesteros, J. A., Shi, L. and Javitch, J. A., 2001, Structural mimicry in G protein-coupled receptors: implications of the high-resolution structure of rhodopsin for structure-function analysis of rhodopsin-like receptors. *Mol. Pharmacol.*, **60**, 1–19.
[5] Pierce, K. L. and Lefkowitz, R. J., 2001, Classical and new roles of beta-arrestins in the regulation of G-protein-coupled receptors. *Nat. Rev. Neurosci.*, **2**, 727–733.
[6] Pierce, K. L., Premont, R. T. and Lefkowitz, R. J., 2002, Seven-transmembrane receptors. *Nat. Rev. Mol. Cell Biol.*, **3**, 639–650.
[7] Limbird, L. E. and Lefkowitz, R. J., 1976, Negative cooperativity among beta-adrenergic receptors in frog erythrocyte membranes. *J. Biol. Chem.*, **251**, 5007–5014.
[8] Jordan, B. A. and Devi, L. A., 1999, G-protein-coupled receptor heterodimerization modulates receptor function. *Nature*, **399**, 697–700.
[9] Rodbell, M., 1995, Nobel Lecture. Signal transduction: evolution of an idea. *Biosci. Rep.*, **15**, 117–133.
[10] Angers, S., Salahpour, A. and Bouvier, M., 2001, Biochemical and biophysical demonstration of GPCR oligomerization in mammalian cells. *Life Sci.*, **68**, 2243–2250.
[11] Angers, S., Salahpour, A. and Bouvier, M., 2002, Dimerization: an emerging concept for G protein-coupled receptor ontogeny and function. *Annu. Rev. Pharmacol. Toxicol.*, **42**, 409–435.
[12] Filizola, M., Olmea, O. and Weinstein, H., 2002, Prediction of heterodimerization interfaces of G-protein coupled receptors with a new subtractive correlated mutation method. *Protein Eng.*, **15**, 881–885.
[13] Rios, C. D., Jordan, B. A., Gomes, I. and Devi, L. A., 2001, G-protein-coupled receptor dimerization: modulation of receptor function. *Pharmacol. Ther.*, **92**, 71–87.
[14] Terrillon, S. and Bouvier, M., 2004, Roles of G-protein-coupled receptor dimerization. *EMBO Rep.*, **5**, 30–34.
[15] Breitwieser, G. E., 2004, G protein-coupled receptor oligomerization: implications for G protein activation and cell signaling. *Circ. Res.*, **94**, 17–27.
[16] Milligan, G., Ramsay, D., Pascal, G. and Carrillo, J. J., 2003, GPCR dimerisation. *Life Sci.*, **74**, 181–188.
[17] Bai, M., 2004, Dimerization of G-protein-coupled receptors: roles in signal transduction. *Cell Signal.*, **16**, 175–186.
[18] Jones, K. A., Borowsky, B., Tamm, J. A., Craig, D. A., Durkin, M. M., Dai, M., Yao, W. J., Johnson, M., Gunwaldsen, C., Huang, L. Y., Tang, C., Shen, Q., Salon, J. A., Morse, K., Laz, T., Smith, K. E., Nagarathnam, D., Noble, S. A., Branchek, T. A. and Gerald, C., 1998, GABA(B) receptors function as a heteromeric assembly of the subunits GABA(B)R1 and GABA(B)R2. *Nature*, **396**, 674–679.
[19] Margeta-Mitrovic, M., Jan, Y. N. and Jan, L. Y., 2001, Ligand-induced signal transduction within heterodimeric GABA(B) receptor. *Proc. Natl Acad. Sci. USA*, **98**, 14643–14648.
[20] Margeta-Mitrovic, M., Jan, Y. N. and Jan, L. Y., 2001, Function of GB1 and GB2 subunits in G protein coupling of GABA(B) receptors. *Proc. Natl Acad. Sci. USA*, **98**, 14649–14654.
[21] Kunishima, N., Shimada, Y., Tsuji, Y., Sato, T., Yamamoto, M., Kumasaka, T., Nakanishi, S., Jingami, H. and Morikawa, K., 2000, Structural basis of glutamate recognition by a dimeric metabotropic glutamate receptor. *Nature*, **407**, 971–977.
[22] Chinault, S. L., Overton, M. C. and Blumer, K. J., 2004, Subunits of a yeast oligomeric G protein-coupled receptor are activated independently by agonist but function in concert to activate G protein heterotrimers. *J. Biol. Chem.*, **279**, 16091–16100.
[23] Guo, W., Shi, L. and Javitch, J. A., 2003, The fourth transmembrane segment forms the interface of the dopamine D2 receptor homodimer. *J. Biol. Chem.*, **278**, 4385–4388.
[24] Baneres, J. L. and Parello, J., 2003, Structure-based analysis of GPCR function: evidence for a novel pentameric assembly between the dimeric leukotriene B4 receptor BLT1 and the G-protein. *J. Mol. Biol.*, **329**, 815–829.
[25] McBee, J. K., Palczewski, K., Baehr, W. and Pepperberg, D. R., 2001, Confronting complexity: the interlink of phototransduction and retinoid metabolism in the vertebrate retina. *Prog. Retin. Eye Res.*, **20**, 469–529.
[26] Polans, A., Baehr, W. and Palczewski, K., 1996, Turned on by Ca2+! The physiology and pathology of Ca(2+)-binding proteins in the retina. *Trends Neurosci.*, **19**, 547–554.
[27] Okada, T., Ernst, O. P., Palczewski, K. and Hofmann, K. P., 2001, Activation of rhodopsin: new insights from structural and biochemical studies. *Trends Biochem. Sci.*, **26**, 318–324.
[28] Baylor, D. A., Lamb, T. D. and Yau, K. W., 1979, Responses of retinal rods to single photons. *J. Physiol.*, **288**, 613–634.
[29] Molday, R. S., 1998, Photoreceptor membrane proteins, phototransduction, and retinal degenerative diseases. The Friedenwald Lecture. *Invest. Ophthalmol. Vis. Sci.*, **39**, 2491–2513.
[30] Humphries, M. M., Rancourt, D., Farrar, G. J., Kenna, P., Hazel, M., Bush, R. A., Sieving, P. A., Sheils, D. M., McNally, N., Creighton, P., Erven, A., Boros, A., Gulya, K., Capecchi, M. R. and Humphries, P., 1997, Retinopathy induced in mice by targeted disruption of the rhodopsin gene. *Nature Genet.*, **15**, 216–219.
[31] Lem, J., Krasnoperova, N. V., Calvert, P. D., Kosaras, B., Cameron, D. A., Nicolo, M., Makino, C. L. and Sidman, R. L., 1999, Morphological, physiological, and biochemical changes in

rhodopsin knockout mice. *Proc. Natl Acad. Sci. USA*, **96**, 736–741.
[32] Filipek, S., Stenkamp, R. E., Teller, D. C. and Palczewski, K., 2003, G protein-coupled receptor rhodopsin: a prospectus. *Annu. Rev. Physiol.*, **65**, 851–879.
[33] Palczewski, K., Kumasaka, T., Hori, T., Behnke, C. A., Motoshima, H., Fox, B. A., Le Trong, I., Teller, D. C., Okada, T., Stenkamp, R. E., Yamamoto, M. and Miyano, M., 2000, Crystal structure of rhodopsin: A G protein-coupled receptor. *Science*, **289**, 739–745.
[34] Okada, T. and Palczewski, K., 2001, Crystal structure of rhodopsin: implications for vision and beyond. *Curr. Opin. Struct. Biol.*, **11**, 420–426.
[35] Teller, D. C., Okada, T., Behnke, C. A., Palczewski, K. and Stenkamp, R. E., 2001, Advances in determination of a high-resolution three-dimensional structure of rhodopsin, a model of G-protein-coupled receptors (GPCRs). *Biochemistry*, **40**, 7761–7772.
[36] Stenkamp, R. E., Filipek, S., Driessen, C. A., Teller, D. C. and Palczewski, K., 2002, Crystal structure of rhodopsin: a template for cone visual pigments and other G protein-coupled receptors. *Biochim. Biophys. Acta*, **1565**, 168–182.
[37] Menon, S. T., Han, M. and Sakmar, T. P., 2001, Rhodopsin: structural basis of molecular physiology. *Physiol. Rev.*, **81**, 1659–1688.
[38] Filipek, S., Teller, D. C., Palczewski, K. and Stenkamp, R., 2003, The crystallographic model of rhodopsin and its use in studies of other G protein-coupled receptors. *Annu. Rev. Biophys. Biomol. Struct.*, **32**, 375–397.
[39] Nair, K. S., Balasubramanian, N. and Slepak, V. Z., 2002, Signal-dependent translocation of transducin, RGS9-1-Gbeta5L complex, and arrestin to detergent-resistant membrane rafts in photoreceptors. *Curr. Biol.*, **12**, 421–425.
[40] Seno, K., Kishimoto, M., Abe, M., Higuchi, Y., Mieda, M., Owada, Y., Yoshiyama, W., Liu, H. and Hayashi, F., 2001, Light- and guanosine 5′-3-O-(thio)triphosphate-sensitive localization of a G protein and its effector on detergent-resistant membrane rafts in rod photoreceptor outer segments. *J. Biol. Chem.*, **276**, 20813–20816.
[41] Elliott, M. H., Fliesler, S. J. and Ghalayini, A. J., 2003, Cholesterol-dependent association of caveolin-1 with the transducin alpha subunit in bovine photoreceptor rod outer segments: disruption by cyclodextrin and guanosine 5′-O-(3-thiotriphosphate). *Biochemistry*, **42**, 7892–7903.
[42] Fotiadis, D., Liang, Y., Filipek, S., Saperstein, D. A., Engel, A. and Palczewski, K., 2003, Atomic-force microscopy: rhodopsin dimers in native disc membranes. *Nature*, **421**, 127–128.
[43] Fotiadis, D., Liang, Y., Filipek, S., Saperstein, D. A., Engel, A. and Palczewski, K., 2004, The G protein-coupled receptor rhodopsin in the native membrane. *FEBS Letters*, **564**, 281–288.
[44] Liang, Y., Fotiadis, D., Filipek, S., Saperstein, D. A., Palczewski, K. and Engel, A., 2003, Organization of the G protein-coupled receptors rhodopsin and opsin in native membranes. *J. Biol. Chem.*, **278**, 21655–21662.
[45] Filipek, S., Krzysko, K. A., Fotiadis, D., Liang, Y., Saperstein, D. A., Engel, A. and Palczewski, K., 2004, A concept for G protein activation by G protein-coupled receptor dimers: the transducin/rhodopsin interface. *Photochem. Photobiol. Sci.*, **3**, 1–12.
[46] Ridge, K. D., Abdulaev, N. G., Sousa, M. and Palczewski, K., 2003, Phototransduction: crystal clear. *Trends Biochem. Sci.*, **28**, 479–487.
[47] Medina, R., Perdomo, D. and Bubis, J., 2004, The hydrodynamic properties of dark and light-activated states of n-dodecyl-[beta]-D-maltoside-solubilized bovine rhodopsin support the dimeric structure of both conformations. *J. Biol. Chem.*, **279**, 39565–39573.
[48] Arimoto, R., Kisselev, O. G., Makara, G. M. and Marshall, G. R., 2001, Rhodopsin-transducin interface: studies with conformationally constrained peptides. *Biophys. J.*, **81**, 3285–3293.
[49] Hamm, H. E., 2001, How activated receptors couple to G proteins. *Proc. Natl Acad. Sci. USA*, **98**, 4819–4821.
[50] Marshall, G. R., 2001, Peptide interactions with G-protein coupled receptors. *Biopolymers*, **60**, 246–277.
[51] Liebman, P. A., Parker, K. R. and Dratz, E. A., 1987, The molecular mechanism of visual excitation and its relation to the structure and composition of the rod outer segment. *Annu. Rev. Physiol.*, **49**, 765–791.
[52] Cone, R. A., 1972, Rotational diffusion of rhodopsin in the visual receptor membrane. *Nat. New Biol.*, **236**, 39–43.
[53] Poo, M. and Cone, R. A., 1974, Lateral diffusion of rhodopsin in the photoreceptor membrane. *Nature*, **247**, 438–441.
[54] Liebman, P. A. and Entine, G., 1974, Lateral diffusion of visual pigment in photoreceptor disk membranes. *Science*, **185**, 457–459.
[55] Saibil, H., Chabre, M. and Worcester, D., 1976, Neutron diffraction studies of retinal rod outer segment membranes. *Nature*, **262**, 266–270.
[56] Downer, N. W. and Cone, R. A., 1985, Transient dichroism in photoreceptor membranes indicates that stable oligomers of rhodopsin do not form during excitation. *Biophys. J.*, **47**, 277–284.
[57] Papermaster, D. S., 1982, Preparation of retinal rod outer segments. *Methods Enzymol.*, **81**, 48–52.
[58] Heuberger, E. H., Veenhoff, L. M., Duurkens, R. H., Friesen, R. H. and Poolman, B., 2002, Oligomeric state of membrane transport proteins analyzed with blue native electrophoresis and analytical ultracentrifugation. *J. Mol. Biol.*, **317**, 591–600.
[59] Papac, D. I., Thornburg, K. R., Bullesbach, E. E., Crouch, R. K. and Knapp, D. R., 1992, Palmitylation of a G-protein coupled receptor. Direct analysis by tandem mass spectrometry. *J. Biol. Chem.*, **267**, 16889–16894.
[60] Hargrave, P. A., 1982, Rhodopsin chemistry, structure and topography. In N. N. Osbourne and G. J. Chader, eds *Progress in Retinal Research* (Pergamon Press, New York), pp. 1–51.
[61] Jap, B. K., Zulauf, M., Scheybani, T., Hefti, A., Baumeister, W., Aebi, U. and Engel, A., 1992, 2D crystallization: from art to science. *Ultramicroscopy*, **46**, 45–84.
[62] Liang, Y., Fotiadis, D., Maeda, T., Maeda, A., Modzelewska, A., Filipek, S., Saperstein, D. A., Engel, A. and Palczewski, K., 2004, Rhodopsin signaling and organization in heterozygote rhodopsin knockout mice. *J. Biol. Chem.*, **279**, 48189–48196.
[63] Schägger, H. and von Jagow, G., 1991, Blue native electrophoresis for isolation of membrane protein complexes in enzymatically active form. *Anal. Biochem.*, **199**, 223–231.
[64] Lee, S. P., O'Dowd, B. F. and George, S. R., 2003, Homo- and hetero-oligomerization of G protein-coupled receptors. *Life Sci.*, **74**, 173–180.
[65] Okada, T., Le Trong, I., Fox, B. A., Behnke, C. A., Stenkamp, R. E. and Palczewski, K., 2000, X-Ray diffraction analysis of three-dimensional crystals of bovine rhodopsin obtained from mixed micelles. *J. Struct. Biol.*, **130**, 73–80.
[66] Janz, J. M. and Farrens, D. L., 2004, Rhodopsin activation exposes a key hydrophobic binding site for the transducin alpha-subunit C-terminus. *J. Biol. Chem.*, **279**, 29767–29773.
[67] Downer, N. W., 1985, Cross-linking of dark-adapted frog photoreceptor disk membranes. Evidence for monomeric rhodopsin. *Biophys. J.*, **47**, 285–293.
[68] Hermanson, G. T., 1996, *Bioconjugate techniques* (Academic Press, San Diego).
[69] Cobb, C. E. and Beth, A. H., 1990, Identification of the eosinyl-5-maleimide reaction site on the human erythrocyte anion-exchange protein: overlap with the reaction sites of other chemical probes. *Biochemistry*, **29**, 8283–8290.
[70] Barclay, P. L. and Findlay, J. B., 1984, Labelling of the cytoplasmic domains of ovine rhodopsin with hydrophilic chemical probes. *Biochem. J.*, **220**, 75–84.
[71] Imamoto, Y., Kataoka, M., Tokunaga, F. and Palczewski, K., 2000, Light-induced conformational changes of rhodopsin probed by fluorescent alexa594 immobilized on the cytoplasmic surface. *Biochemistry*, **39**, 15225–15233.
[72] Ovchinnikov Yu, A., Abdulaev, N. G. and Bogachuk, A. S., 1988, Two adjacent cysteine residues in the C-terminal

cytoplasmic fragment of bovine rhodopsin are palmitylated. *FEBS Letters*, **230**, 1–5.
[73] Gelasco, A., Crouch, R. K. and Knapp, D. R., 2000, Intrahelical arrangement in the integral membrane protein rhodopsin investigated by site-specific chemical cleavage and mass spectrometry. *Biochemistry*, **39**, 4907–4914.
[74] Cai, K., Klein-Seetharaman, J., Hwa, J., Hubbell, W. L. and Khorana, H. G., 1999, Structure and function in rhodopsin: effects of disulfide cross-links in the cytoplasmic face of rhodopsin on transducin activation and phosphorylation by rhodopsin kinase. *Biochemistry*, **38**, 12893–12898.
[75] Yang, K., Farrens, D. L., Altenbach, C., Farahbakhsh, Z. T., Hubbell, W. L. and Khorana, H. G., 1996, Structure and function in rhodopsin. Cysteines 65 and 316 are in proximity in a rhodopsin mutant as indicated by disulfide formation and interactions between attached spin labels. *Biochemistry*, **35**, 14040–14046.
[76] Yu, H., Kono, M. and Oprian, D. D., 1999, State-dependent disulfide cross-linking in rhodopsin. *Biochemistry*, **38**, 12028–12032.
[77] Saxton, W. O., 1996, Semper: Distortion compensation, selective averaging, 3-D reconstruction, and transfer function correction in a highly programmable system. *J. Struct. Biol.*, **116**, 230–236.

Received 21 September 2004; and in revised form 27 October 2004.